Pathogenic Murine Coronaviruses

I. Characterization of Biological Behavior *in Vitro* and Virus-Specific Intracellular RNA of Strongly Neurotropic JHMV and Weakly Neurotropic A59V Viruses

JAMES A. ROBB[1] AND CLIFFORD W. BOND[2]

Department of Pathology, M-012, University of California, San Diego, La Jolla, California 92093

JHM virus (JHMV) and A59 virus (A59V) are neurotropic members of the hepatoencephalitis group of murine coronaviridae. JHMV has a markedly greater neurotropism for weanling BALB/c mice than does A59V. Both viruses display one-hit kinetics when grown *in vitro* in 17CL-16 cells, a clone of BALB/c3T3 cells. Virus-specific intranuclear, cytoplasmic, and surface antigens have been observed for both viruses by immunofluorescence. The intranuclear antigen appears first at about 2 hr after infection (hpi) followed by the development of the cytoplasmic and surface antigens at 3 hpi at 38.5°. Most, if not all cells that develop the intranuclear antigen, produce cytoplasmic antigen and presumably progeny virus. Progeny virus production is independent of cell fusion and formation of syncytia. Virus-specific ribonucleoprotein is synthesized in the presence of 1 μg/ml actinomycin D, a concentration sufficient to inhibit the synthesis of cellular ribonucleoprotein species that have sedimentation properties similar to the virus-specific species. The virus-specific ribonucleoprotein species that is resistant to 10 mM EDTA, presumptive virion ribonucleoprotein, has a sedimentation value in sucrose of about 230 S for JHMV and 200 S for A59V. The species of virus-specific ribonucleoprotein that are sensitive to 10 mM EDTA, presumptive messenger ribonucleoprotein, are about 40–100 S in sucrose for both viruses. The purified presumptive virion RNA is about 50 S in sucrose for both viruses. The major species of presumptive mRNA of both viruses is about 18 S with secondary species of about 28 S in sucrose. Denaturation of the virus-specific RNA with heat and dimethylsulfoxide does not appreciably alter the sedimentation profiles of either the presumptive virion RNA or mRNA species.

INTRODUCTION

The molecular mechanisms underlying the pathogenesis of many virus-caused diseases in humans and mammals are poorly understood at present (Fenner and White, 1976; Robb, 1977b). We are investigating the molecular mechanisms that underlie the pathogenesis of the diseases produced in mice by the murine hepatoencephalitis group of coronaviradae: encephalitis; demy-

elination; hepatitis; and interstitial pneumonitis (see Piazza, 1969, McIntosh, 1974, and Robb and Bond, 1979 for review). Our interest is focused on the demyelination produced in the central nervous system of mice that have been infected by neurotropic members of this group of viruses.

JHM virus (JHMV) is one member of this group of viruses that has a strong neurotropism after intranasal or intracerebral inoculation, but not after intraperitoneal or subcutaneous inoculation. JHMV was isolated and partially characterized by Cheever *et al.* in 1949 from a mouse with flaccid hindlimb paralysis. The virus was named JHM in honor of Professor J. Howard

[1] To whom reprint requests should be addressed at the Department of Pathology, The Green Hospital of Scripps Clinic La Jolla, Calif. 92037.

[2] Present address: Department of Microbiology, University of Montana, Bozeman, Mont. 59715.

Mueller in the Department of Bacteriology and Immunology at Harvard, the mentor of the virus' isolators. Most susceptible weanling mice die of acute panencephalitis within a few days after intracerebral or intranasal inoculation with JHMV. The surviving animals usually develop a primary demyelination within 2 weeks after inoculation (Bailey *et al.*, 1949; Lampert *et al.*, 1973; Weiner, 1973). The neuropathology was described by Bailey *et al.* 1949. The cause of the primary demyelination is a direct cytocidal effect of the virus on infected oligodendroglia (Weiner, 1973; Lampert *et al.* 1973). Oligodendrocytes are the neural cells responsible for the synthesis and maintenance of the myelin sheath that surrounds axons. This myelin sheath permits the efficient conduction of electrical impulses along the axon. The mechanism(s) of the virus' cytocidal effect is not known at present. Remyelination of the denuded axon is accomplished in animals surviving the primary demyelination by proliferation of noninfected oligodendrocytes and re-sheathing of the denuded axons by the proliferated oligodendrocytes (Herndon *et al.*, 1977). Occasional animals have recurrent bouts of demyelination and remyelination, but little is known about the pathogenesis of this recurrent demyelination. A persistent infection with JHMV may be involved in this recurrent demyelination.

A biochemical comparison of JHMV with weakly neurotropic members of the group should help elucidate the molecular mechanisms underlying the primary demyelination and encephalitis produced in weanling mice by JHMV infection (see Robb and Bond, 1979). A major difficulty with studying the *in vitro* replication of coronaviruses has been the difficulty of growing these viruses to sufficient titer. In fact, the replication strategy of the murine coronaviridae is not yet known. We describe in this paper the *in vitro* system we have optimized for growth of JHMV and a closely related weakly neurotropic murine coronavirus, A59V. We have also characterized the intracellular virus-specific species of presumptive virion RNA and mRNA. The accompanying papers describe the proteins of JHMV and A59V (Bond *et al.*, 1979) and the characterization of temperature-sensitive mutants of JHMV (Robb, *et al.*, 1979).

MATERIALS AND METHODS

Biohazard containment. All work with infectious virus is done in Class I Baker Sterilgard laminar flow hoods using P2 containment according to the NIH Recombinant DNA Guidelines (Fredrickson, 1976).

Cells and media. Three murine cell lines were grown at 33° using Dulbecco–Vogt Modified Eagle's medium supplemented with 2.0 g/liter glucose, 25 mg/liter chlortetracycline–HCL (Sigma), and 10% fetal bovine serum (FBS), and buffered at pH 7.4 with 2.0 g/liter NaHCO$_3$ and 15 mM each of HEPES (N-2-hydroxyethylpiperazine-N'-2-ethanesulfonic acid), Mops (morpholinopropanesulfonic acid), and Tes [N-tris-(hydroxymethyl)methyl - 2 - aminoethane - sulfonic acid]. This medium is called DEB10. The three murine lines investigated were NCTC 1469 (Evans *et al.*, 1952), DBT (Hirano *et al.*, 1974), and 17Cl-1 derived from the BALB/3T3 line (Sturman and Takemoto, 1972).

Virus infection. The JHM strain of mouse hepatitis virus was originally isolated by Cheever *et al.* (1949) from a Schwenker Swiss white mouse with flaccid paralysis. We are using isolate No. 718 provided by Dr. Janet Hartley (Hartley and Rowe, 1963) as a frozen 10% suspension of weanling mouse brain. This isolate was passaged 46 times as a 10% brain suspension using intracerebral injections in Swiss–Webster weanling mice before we introduced it into cell culture. The weakly neurotropic MHV-A59 (A59V) strain of *in vitro*-adapted mouse hepatitis virus was provided by Dr. Lawrence Sturman (Sturman and Takemoto, 1972). The rationale for the following infection procedure we adopted is provided under Results. 17CL-1 cells were removed from the plastic substrate with 0.05% twice-crystallized trypsin–0.02% EGTA [ethylene glycolbis(β-aminoethyl ether) N,N'-tetraacetic acid], suspended in DEB2 (2% FBS), centrifuged at 500 g for 2 min, and resuspended in DEB2 at the appropriate

multiplicity of infection (m.o.i.). Virus stocks were grown at 33° using an m.o.i. of 10^{-4}. Virus adsorption was at a cell concentration of 5×10^6/ml of DEB2. The virus–cell mixture was plated into appropriate vessels with additional DEB2 after a 30-min adsorption period at 33 or 37°, with agitation every 5 min to keep the cells in suspension. For virus harvests, infected cells were scraped with a sterile rubber policeman, sonically disrupted for 30 sec at 80 ws (peak envelope power) in ice water using tightly capped test tubes in the cup probe of a Biosonik IV cell disruptor, clarified at 733 g for 5 min, and titered immediately or stored at $-70°$. Sonic disruption is not necessary if the infected cells are harvested after 24 hr of infection.

Virus titration. We have adopted an endpoint dilution microtitration procedure that has been previously described for animal viruses (Robb, 1973). The rationale for this choice is given under Results. 17CL-16 cells are used in the titration. Wells are examined at 48 hr after infection (hpi) for the formation of typical syncytia. The infectious units per milliliters (iU/ml) are calculated from the Poisson distribution.

Cloning of virus. JHMV and A59 were doubly cloned at 38.5° by the endpoint dilution technique in Microtest plates. The chance of two infecting virions being present in the same well was 0.00001% (10^{-7}).

Cloning of cells. One hundred cells were placed in a Falcon T-30 flask and allowed to form clones in DEB10C (10% calf serum) at 38.5°. When the clones were 1–3 mm in diameter, the medium was aspirated, the clones rinsed once with DEB0 (no FBS), and 6 ml of 0.5% Noble agar (Difco) in Puck's saline A containing 0.05% trypsin (2× crystallized) and 0.02% EGTA at 40° was added. After 15 min at 20°, isolated clones were picked by the following technique. A sterile Pasteur pipet was heated at its large end and used to melt a hole in the top of the T-30 flask over the clone to be picked. A second sterile Pasteur pipet was then inserted through the hole, and the clone with its attendant agar was carefully sucked up and mixed into 1 ml DEB10C in a MultiWell well. The selected

clones were grown into stocks at 38.5° and stored in liquid nitrogen.

Immunofluorescent and immune electron microscopy. Mouse anti-JHMV and anti-A59V sera were prepared by injecting thirty 4-week-old BALB/c mice intraperitoneally with 1000 iU of doubly cloned wild-type JHMV or A59V. Two weeks after infection, the animals were exsanguinated and their sera pooled. These antisera are polyspecific and recognize seven virus-specific proteins in infected cells as assayed by radioimmune recipitation (Bond *et al.*, 1979). Mock-, JHMV-, and A59V-infected cells were fixed with absolute methanol and stained with the indirect immunofluorescent technique previously described (Robb, 1977a) using 0.2 ml per dish of mouse anti-JHMV or anti-A59V serum at a 1:4 dilution with PBS (pH 7.4), 0.2 ml of fluorescein isothiocyanate-conjugated goat anti-mouse-IgG IgG, at a 1:8 dilution with PBS (pH 7.4). After a 30-min incubation at room temperature, the dishes were rinsed twice with 2 ml PBS (pH 7.4) and examined. The method of Ash and Singer (1976) was used for the immunofluorescence of formaldehyde-fixed, Triton X-100-extracted cells. Using this method, infected cells in 32-mm petri dishes were placed on an ice-water mixture and rinsed once with cold DEB0 (no FBS). Two milliliters of cold 2% formaldehyde was added and the dishes were kept for 20 min on the ice-water mixture. The following steps were performed at room temperature. The formaldehyde was removed, and the cells were rinsed once with 1 ml 50 mM NH_4Cl with swirling every 30 sec for 5 min. After decanting the NH_4Cl solution, the cells were rinsed twice with 2 ml PBS (pH 7.4) with swirling every 30 sec for 5 min each. After decanting the final rinse solution, 1 ml of 0.1% Triton X-100 was added for 4 min. After removal of the Triton X-100, the cells were rinsed twice with 2 ml PBS (pH 7.4) with swirling every 30 sec for 5 min each. The cells were then immunofluorescently stained in the same manner as the cells fixed with absolute methanol.

Virus-specific surface antigen was detected on living cells by the following

technique. The 32-mm petri dishes with infected cells were placed in ice water and rinsed once with cold DEB0 (no FBS). Then 0.2 ml of mouse anti-JHMV serum, diluted 1:4 with DEB0, was added per dish, and the dishes were agitated every 2 min. After 5 min, the dishes were rinsed once with cold DEB0 and fixed with cold 2% formaldehyde for 20 min on ice water. After aspiration, 1 ml of 50 mM NH_4CL was added and aspirated. The dishes were rinsed twice with 2 ml PBS (pH 7.4) and immuno-fluorescently stained by the indirect method described.

Infected cells were also prepared in suspension for immune electron microscopy of the virus-specific surface antigen by removing the cells from the plastic dishes floating on ice water with cold 0.1% EGTA in Puck's saline A. The suspended cells were then rinsed once with cold DEB0 and processed in a manner similar to the method for attached cells with the following exceptions: The cells were pelleted at 400 g × 2 min at 18° before each aspiration; and ferritin-conjugated rabbit anti-mouse-IgG IgG (Cappel Laboratories), used at a dilution of 1:4 with PBS (pH 7.4), replaced the fluorescein isothiocyanate-conjugated goat anti-mouse-IgG IgG. The ferritin-labeled cells were rinsed six times with PBS (pH 7.4) before being prepared for electron microscopy (Lampert et al., 1975).

The immunofluorescently stained cells were examined using a Leitz Dialux fluorescent microscope equipped with both transmitted halogen and incident mercury light, FITC filters, and a Leitz dry dark-field condensor. A Leitz Orthomat II automatic 35-mm camera, Kodak Tri-X film, and an Olympus 40X water immersion objective were used to photograph the fluorescing cells.

Virus-specific intracellular ribonucleoprotein (RNP) and RNA. Cells were either infected with a lysate of 17CL-16 cells (mock) or with virus at a m.o.i. = 0.10. After a 30-min adsorption period at 37°, the cells were plated into 150-mm plastic petri dishes (Falcon) using 5–7 × 10⁷ cells per dish and 10 ml DEB2. After 4 hr of incubation at 38.5°, the restrictive temperature for

the temperature-sensitive mutants of JHMV described in a following paper (Robb et al., 1979), 1 µg/ml of actinomycin D (Merck) was added. After a further 15-min incubation at 38.5°, 50–100 µCi/ml of 5'-[³H]-uridine (New England Nuclear, 106 mCi/mg) was added. After a further 2-hr incubation at 38.5°, the ribonucleoprotein was extracted in the following manner. The petri dishes were set in an ice-water mixture and aspirated. Each dish was rinsed once with 20 ml cold sterile reticulocyte standard buffer (RSB pH 7.4): 10 mM NaCl; 10 mM Tris; and 1.5 mM $MgCl_2$. After aspiration, 3 ml cold sterile RSB with 1% Nonidet-P40 (NP40) was added. After gentle Pasteur pipetting, the extraction mix was centrifuged at 1100 g for 2 min at 4°. Fractionation of the RNP was accomplished by centrifuging 1.5 ml of the extracted material on a 10–30% (w/w) equal mass sucrose–sterile RSB gradient (10%: 8.0 ml weighing 8.32 g; 30%: 7.4 ml weighing 8.32 g) using 15.4 ml sucrose–RSB per tube in a SW 27.1 rotor at 27,000 rpm at 4° for 150 min in a Beckman L3-50 ultracentrifuge. Polysomes were disrupted before the sucrose–RSB centrifugation by the technique of Penman et al. (1968) using 10 mM EDTA (30 µl 0.5 M sterile EDTA, pH 7.4) in one-half (1.5 ml) of the extracted sample. Sterile deionized water, 30 µl, was added to the other 1.5 ml of extracted sample. Fractions of 0.5 ml were collected from the bottom of the tube being sure to keep the fractions immersed in an ice-water mixture during fraction collection. The pellet was resuspended in 0.5 ml 0.1% sodium dodecyl sulfate (SDS) in SDS buffer (see below). Aliquots, 50 µl, were taken from each fraction using sterile plastic tips and an Eppendorf syringe and extracted with 10% trichloroacetic acid. The radio-activity precipitated on glass-fiber filters was measured with a Beckman LSC-100 counter using minivials and 2.0 ml scintillation fluid per vial.

For RNA analysis only, the fractions were pumped at room temperature directly into tubes that contained the following ribonuclease inactivation mixture: 1/10 vol sterile 4 M NaCl; 1/10 vol 10% SDS; 1/10 vol

0.1 M EDTA; and 7 mg/ml Proteinase K (Fungal, EM Biochemicals). One drop of yeast RNA, 4 mg/ml, was added as carrier RNA, 100 μl aliquots were treated with 10% trichloroacetic acid, and the precipitated radioactivity, collected on glass-fiber filters, was measured with a Beckman LSC-100 counter using minivials and 2 ml scintillation fluid per vial. The single or pooled fractions were then extracted with room temperature phenol. An equal volume (not exceeding 2 ml) of 80% phenol with 0.01 M EDTA was added to each sample and the mixture gently vortexed. A volume of 1% isopentyl alcohol in chloroform equal to the original RNA sample volume (not exceeding 2 ml) was then added and the mixture again gently vortexed. The mixture was then centrifuged at 278 g at 4° for 2 min and the bottom component was removed with a Pasteur pipet. This procedure was repeated once more. A volume of 1% isopentyl alcohol in chloroform equal to the original sample was then added. The mixture was gently vortexed and centrifuged at 278 g at 4° for 2 min. The bottom component was removed with a Pasteur pipet and the procedure repeated once more. "Phenol-extracted" yeast RNA, 1/100 vol, was added as carrier. After adding twofold the volume of the original RNA sample of 95% ethanol at −20°, the mixture was vortexed and stored for at least 12 hr at −20°. The precipitated, deproteinized RNA was collected by centrifugation at 27,000 g at −10° for 20 min and redissolved in 0.1% SDS or denatured with dimethyl sulfoxide (DMSO) in the following manner. The precipitated RNA was resuspended in 0.1 ml DMSO containing 1% sterile 0.01 M Tris, pH 7.4. After being kept in a 37° water bath for 5 min with agitation every minute, 0.2 ml of 0.1% SDS buffer (0.01 M NaCl, 0.01 M Tris, pH 7.4, and 0.001 M EDTA) was added and the mixture vortexed. The mixture was then treated for 1 min at 68°. The native and denatured RNA were then analyzed on a 10–30% equal mass sucrose–0.1% SDS in SDS buffer gradient by applying 0.10-ml samples on a 5.0-ml gradient in a SW50.1 rotor at 46,000 rpm for 107 min at 20° in a Beckman L3-50 ultra-centrifuge. The fractions were collected from the bottom directly into minivials using 0.16-ml fractions. Deionized water, 0.2 ml, and 3 ml Aquasol I were added to each vial. After vortexing the mixture to clarity, the samples were counted in a Beckman LSC-100 counter.

RESULTS

Choice of Cell Line

JHMV replicated in three murine cell lines: 17CL-1, NCTC 1469, and DBT. Replication was not detected in more than 20 independent clones of simian virus 40-transformed BALB/3T3 cells, or in several murine, hamster, rat, canine, simian, and human lines. Although syncytial plaques were detectable without an agarose overlay at 24 hr after infection in infected DBT cells, the virus did not propagate further and noninfected cells "healed" the plaque in 2–3 days. Plaque production and propagative infection occured in NCTC 1469 cells, but reproducible results were hard to achieve on a day-to-day basis. Titration of a single pool of virus varied more than 10-fold when measured using different pools and passage levels of NCTC 1469 cells. The 17CL-1 line of BALB/3T3 cells was chosen for two reasons. The cells grow well in culture flasks, microtest plates, petri dishes, and roller bottles. Titration and growth of virus are reproducible with different pools and different passage levels of these cells at both 33 and 38.5°.

Selection of a Subclone of 17CL-1

Subcloning of the original 17CL-1 cells was necessary because about 50% of the 17CL-1 cells did not adsorb virus as detected by membrane immunofluorescence at the end of the 30-min adsorption period at 38.5°. This virus-specific immunofluorescence disappeared by 60 min after infection at 38.5°. Furthermore, this "early" membrane-associated fluorescence was in clumps and appeared to migrate into the Golgi region between 30–60 min after infection at 38.5° in contrast to the finely granular virus-specific membrane-associated

immunofluorescence that appeared on lamellapodie at about 3–4 hpi.

Ten clones were picked: three with a somewhat fibroblastic morphology; four with an epitheloid morphology; and three which formed multinucleated giant cells that did not contain JHMV or A59V antigens by immunofluorescence or infectious JHMV or A59V by direct infectivity assays. The clones were tested for the maximum yield of JHMV and A59V, their sensitivity to syncytia formation by JHMV and A59V (titer of a single pool of virus in all clones), ease in recognizing syncytia formed by JHMV and A59V in microtitering, and sensitivity to infection by JHMV and A59V grown in an individual clone and subsequently titered in that clone. The only significant differences noted, as compared to the original 17CL-1 cells, were that three clones, one of each morphology, had delayed CPE and took about 20 hr longer at 38.5° to reach their maximum yield, and that one fibroblastic clone formed syncytia that were more readily recognized. This fibroblastic clone with "easy-to-read" syncytia (see Fig. 4) is designated 17CL-16 (the sixth subclone derived from the first original clone).

Choice of Titration Conditions

Preparation of cells, type of serum, concentration of serum, pH of medium, concentration of cells, volume of virus–cell suspension, and length of incubation were investigated to develop an optimal endpoint dilution microtitration technique. The removal of cells from the plastic substrate with 0.05% trypsin–0.02% EGTA, 0.02% EGTA plus scraping, or scraping alone had little effect on either the subsequent yield of virus from the cells or on the titer when the different cell preparations were used for titration. The trypsin–EGTA procedure was chosen because it is easy and produces more than 99% single cells. Calf serum and FBS were compared at 10, 5, 2, 1, and 0.5% concentrations. The calf serum was inhibitory at all concentrations compared to the FBS. The reason for this inhibition is not known at present. The 2% concentration of FBS produced the optimal titer. The pH of the medium was investigated from 6.5 to 7.8. The titer was reduced at the high and low pH values. A pH of 7.4 was chosen. The concentration of cells was investigated from 5×10^4/ml to 5×10^6/ml. A concentration of 5×10^5/ml produced optimal titers with very good reproducibility. The volume of virus–cell suspension was investigated at 2, 5, and 10 μl/well and no differences were observed. The 2 μl/well volume was chosen for conservation of virus, cells, and medium. The length of incubation was investigated at 24, 48, and 72 hpi at 33 and 38.5°. A maximum titer was observed at 48 hpi at both temperatures. Plaque assays using 0.75% agarose gave the same titers as did the endpoint dilution microtitration techniques.

Storage of JHMV and A59V

The infectivity of JHMV and A59V in clarified, infected cell lysates containing DEB2 was monitored during various storage conditions. Infectivity was very stable to freeze–thaw as the titer was unchanged after eight cycles of freeze–thaw at −70°. The following losses of infectivity were observed during continuous storage: 50%/year at −70°; 50%/month at −40°; 90%/week at −20°; and 50%/week at 4°.

One-Hit Kinetics of JHMV and A59V Infections

Figure 1 demonstrates one-hit kinetics of infection for JHMV and A59V.

Temporal Appearance of JHMV and A59V Infected Cells

The data in Fig. 2 show that the number of infected cells, as detected by immunofluorescence, reaches a maximum at about 4–5 hr after infection at 38.5°. The maximum number of detectable infected cells is in good agreement with the number predicted from the Poisson distribution using 0.10 iU per cell: Ten percent of the cells should receive one or more virions. The virus-specific intranuclear stippling (Fig. 3) precedes the appearance of detectable cyto-

plasmic and Golgi fluorescence (Fig. 2). Most, if not all cells that produce intra-nuclear stippling go on to produce cyto-plasmic fluorescence and probably progeny virus (Fig. 2). Detectable cytoplasmic fluorescence in methanol-fixed cells precedes the appearance of particulate fluorescence in the Golgi region in formaldehyde-fixed, Triton-extracted cells by about 30–60 min at 38.5°.

Percentage of Infected Cells, Yield of Infectious Virus, and "Burst Size" as a Function of the Multiplicity of Infection

Virus multiplication may be inhibited when cells are infected at high multiplicity (Huang and Baltimore, 1970). High multi-plicity experiments however, facilitate biochemical investigations of viral-specific nucleic acid and protein synthesis because the majority of the cells are synchronously infected. The data in Table 1 show that the percentage of infected cells predicted by the Poisson distribution is realized for multi-plicities below 0.4 for JHMV and 0.6 for A59V. Above these values, an inhibition of infection occurs as detected by immuno-fluorescence. The maximal yield of infectious virus, however, is *independent* of the multiplicity. These data suggest that the number of infectious virus produced by a single infected cell is decreased as the multiplicity is increased, i.e., the burst size

FIG. 2. Temporal appearance of JHMV- and A59V-infected 17CL-16 cells at 38.5° as detected by virus-specific immunofluorescence. Cells were infected with a multiplicity of 0.10 in 32-mm petri dishes and fixed at the indicated times with methanol before immunofluorescent staining with mouse anti-JHMV or anti-A59V. (O) JHMV- and (□) A59V-infected cells having *only* intranuclear fluorescence; total number of (●) JHMV- or (■) A59V-infected cells, i.e., both nuclear-positive and cytoplasmic/nuclear-positive cells were counted.

is *dependent* upon the multiplicity. The reduction in burst size begins to stabilize at the multiplicity where the inhibition of intracellular fluorescence begins. Although the virus stocks have defective particles present, these defective particles seem to have little "interfering" potential because there is no reduction in the number of progeny-infectious virus during 40 serial undiluted passages of these viruses in the 17CL-16 cells (Robb, unpublished observa-tion). The mechanism of the multiplicity-dependent burst size is currently not known. The data in Table 1 also show that the maximum yield of virus occurs within 12 hpi at 38.5° and then has a multiplicity-dependent decrease with time.

Progeny Virus Production is Independent of Intercellular Fusion (Syncytial Formation)

The data in Table 1, showing that the maximal yield of progeny virus was independent of the multiplicity, suggested that intercellular fusion produced by the virus infection may not be necessary for the production of progeny virus. If amplification
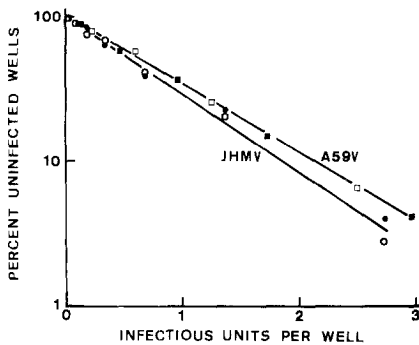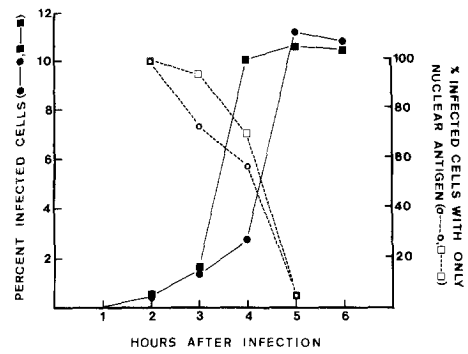

FIG. 1. One-hit kinetics of infection for JHMV and A59V in 17CL-16 cells at 33°. Four microtest plates were infected at each virus dilution producing 240 wells per point. Two independent experiments are shown for each virus: JHMV (●, O) and A59V (■, □).

of progeny virus production occurred by the recruitment of uninfected cells into infected syncytia, then the burst size of infected cells in sparse culture, where syncytial formation is markedly inhibited due to the distance between cells, should be proportionately smaller than the maximal yield from infected cells in dense culture. To test this prediction, a pool of 17CL-16 cells was infected with a low multiplicity and then diluted into replicate 32-mm petri dishes. The subsequent burst size was then determined as shown in Table 2. These data clearly show that recruitment of uninfected cells into syncytia does not amplify the number of progeny virus producing a larger burst size. In addition, we have isolated temperature-sensitive mutants that do not form syncytia at 38.5°, and that have no reduction in the virus yield at 38.5° as compared to the yield at 33° (Robb *et al.*, 1979). All of these observations demonstrate that syncytia formation is not necessary for the production of progeny virus and, moreover, that the progeny virus are probably primarily produced in the cell that is initially infected. The reason for the reduced burst size of JHMV-infected cells during sparse and dense culture, but not during infection in the intermediate cell concentrations, has yet to be determined.

Morphology of JHMV and its Cytopathic Effect in 17CL-16 cells

Figure 4 demonstrates the formation of syncytia typical of JHMV and A59V infection at 33 and 38.5°. The JHMV syncytia contain 10–20 nuclei at the time they peel off the plastic while those produced by A59V contain fewer nuclei, 3–10. Adjacent syncytia do not coalesce to form larger syncytia with centrally located nuclei. Figure 5 demonstrates the typical budding of JHMV ribonucleoprotein into cisternae of the endoplasmic reticulum as examined by transmission electron microscopy. A59V has a similar budding mechanism in 17CL-16 cells at both 33 and 38.5°.

JHMV- and A59V-specific antigen(s) is present on the surface of infected living cells by 4 hpi at 38.5° when the cells are examined by immunofluorescence using anti-JHMV or anti-A59V serum (Fig. 6). This virus-specific surface antigen can also be demonstrated by transmission electron microscopy using ferritin-labeled rabbit anti-mouse-IgG IgG (Fig. 6). Nucleocapsids have not been detected beneath the plasma membrane. Studies are presently underway to identify this antigen(s) by radioimmune precipitation and polyacrylamide slab gel electrophoresis and to determine whether "capping" of this virus-specific plasma membrane-associated antigen(s) can be detected. The identification and function of the intranuclear antigen observed in methanol-fixed cells are being investigated.

Virus-Specific Intracellular Ribonucleo-Protein (RNP) and RNA

Figure 7 shows that A59V-specific RNP, with sedimentation values greater than 40 S, is selectively synthesized in the presence of 1 µg/ml actinomycin D. A59V-specific messenger RNA (mRNA) can, therefore, be defined as that RNA which is synthesized in the presence of 1 µg/ml actinomycin D, is present in the cytoplasmic RNP of infected cells, and as RNP, shifts its sedimentation value from a higher level (mRNP in polyribosomes) to a lower value (free mRNP) in the presence of 10 m*M* EDTA (Penman *et al.*, 1968). Figure 7 shows the results of adding 10 m*M* EDTA to the cytoplasmic RNP of infected cells. A preliminary time-course experiment using 2-hr pulses every 2 hr showed that a pulse from 4–6 hpi gave optimum results at 38.5°. The profiles of mock-infected RNP are the same in the absence and presence of 10 m*M* EDTA. The peak at 200 S is over 95% resistant to the EDTA treatment and is, therefore, the presumptive virion RNP or nucleocapsid. The RNP that shifts from heavier to lighter regions, especially to the 40–100 S region is the presumptive A59V-specific mRNP. The EDTA-sensitive RNP in the pellet (about 60% of the RNP in the pellet) probably represents membrane-associated polyribosomes as demonstrated for Sindbis virus
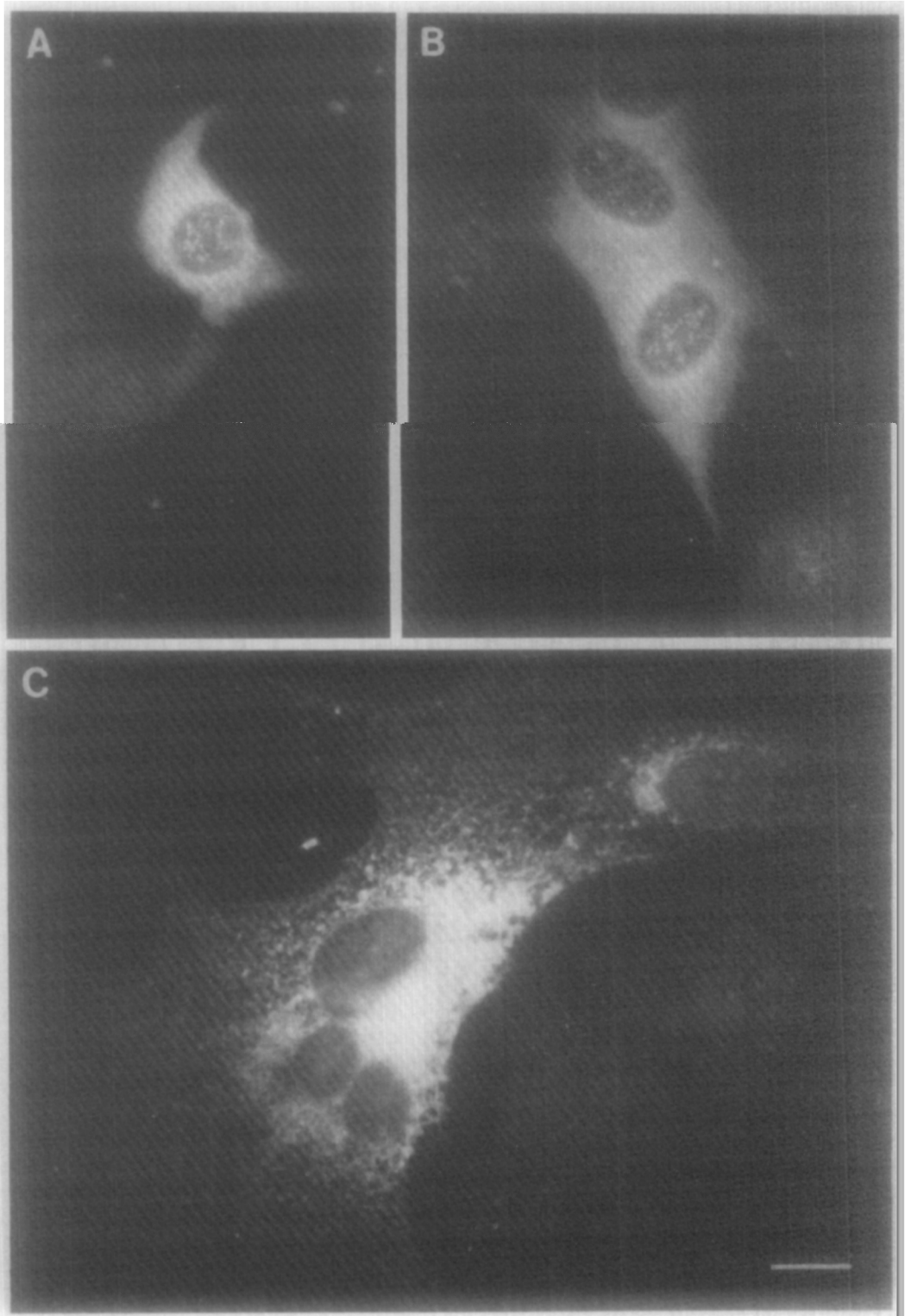
TABLE 1

PERCENTAGE OF INFECTED CELLS, YIELD OF INFECTIOUS VIRUS, AND "BURST SIZE" AS A FUNCTION OF THE MULTIPLICITY OF INFECTING JHMV AND A59V IN 17CL-16 CELLS AT 38.5°.

m.o.i. (iU/cell)	Theoretical percentage infectivity[a]	Percentage FA+ cells[b]	Total virus yield (10^{-6} iU)[c]			Apparent "burst size" (iU/FA+ cell)[d]		
			12 hpi	24 hpi	48 hpi	12 hpi	24 hpi	48 hpi
JHMV								
0.04	4.0	3.6	2.0	1.1	0.10	56	32	2.8
0.12	11	11	1.4	1.1	0.11	13	10	1.0
0.40	33	28	1.4	0.82	0.10	5.0	2.9	0.35
1.2	70	32	1.4	0.95	0.02	4.4	3.0	0.07
4.0	98	45	1.5	0.72	0.01	3.3	1.6	0.02
12	100	53	0.9	0.73	0.02	1.7	1.4	0.04
A59V								
0.02	2.0	2.0	35	21	0.58	1750	1050	29
0.06	5.8	6.3	23	16	0.08	365	254	1.2
0.20	18	17	18	11	0.03	106	65	0.2
0.60	45	42	35	8.2	0.02	83	20	0.05
2.0	86	51	27	4.3	0.02	53	8.4	0.04
6.0	99	73	37	5.0	0.01	53	6.8	0.01
20	100	77	42	8.3	0.03	55	11	0.04

[a] Percentage of cells receiving one or more infectious units (virions) calculated from the Poisson distribution.

[b] Cells were methanol fixed at 5 hpi (see Figs. 1 and 2) and stained with mouse anti-JHMV or anti-A59V, respectively. Five hundred cells were counted in each of three separate regions of the 32-mm petri dish. The *maximum* standard error of the mean was ±21%. A separate independent experiment gave values within the maximum standard error of the mean. Each petri dish contained 10^6 cells.

[c] The amount of virus produced by 12, 24, or 48 hpi in duplicate 32-mm petri dishes (16^6 cells/dish) for each value. The maximum standard error of the mean was ±47%. A separate independent experiment gave values within the maximum standard error of the mean.

[d] "Burst size" is defined by the ratio, total virus yield/No. of FA+ cells.

by Wirth *et al.* (1977), a prediction that is being investigated.

The data in Figure 8 characterize the deproteinized RNA in pooled material from the "heavy" (presumptive nucleocapsid) and "light" (presumptive mRNP) regions of the gradients shown in Fig. 7. The RNA profiles (Figs. 8A and B) are affected very little by the DMSO denaturation (Figs. 8C and D). A loss of RNA (presumptive

FIG. 3. Intranuclear and cytoplasmic JHMV- and A59V-specific antigens in 17CL-16 cells. Cells were infected with an m.o.i. of 0.1 and incubated at 38.5° for 4 hr. They were either fixed with methanol (A, B) or formaldehyde–Triton (C) before staining with polyspecific mouse anti-JHMV or anti-A59V. The photographs are of JHMV-infected cells. The immunofluorescent staining patterns are similar for both JHMV and A59V using virus-specific antiserum and in reciprocally stained preparations. The pattern is the same at 33°. The sequence of syncytial formation is cell–cell contact (A), intercellular fusion (B), and continued recruitment of uninfected cells (C). The intranuclear stippling appears to be predominantly in the perinucleolar regions. The intranuclear and ground-glass cytoplasmic antigens are lost after formaldehyde–Triton treatment. The fluorescence remaining after formaldehyde–Triton treatment appears to be in the Golgi apparatus and endoplasmic reticulum, the site of virus budding. Golgi apparatuses appear to coalesce during syncytial formation (C). The scale bar in C is 10 µm.
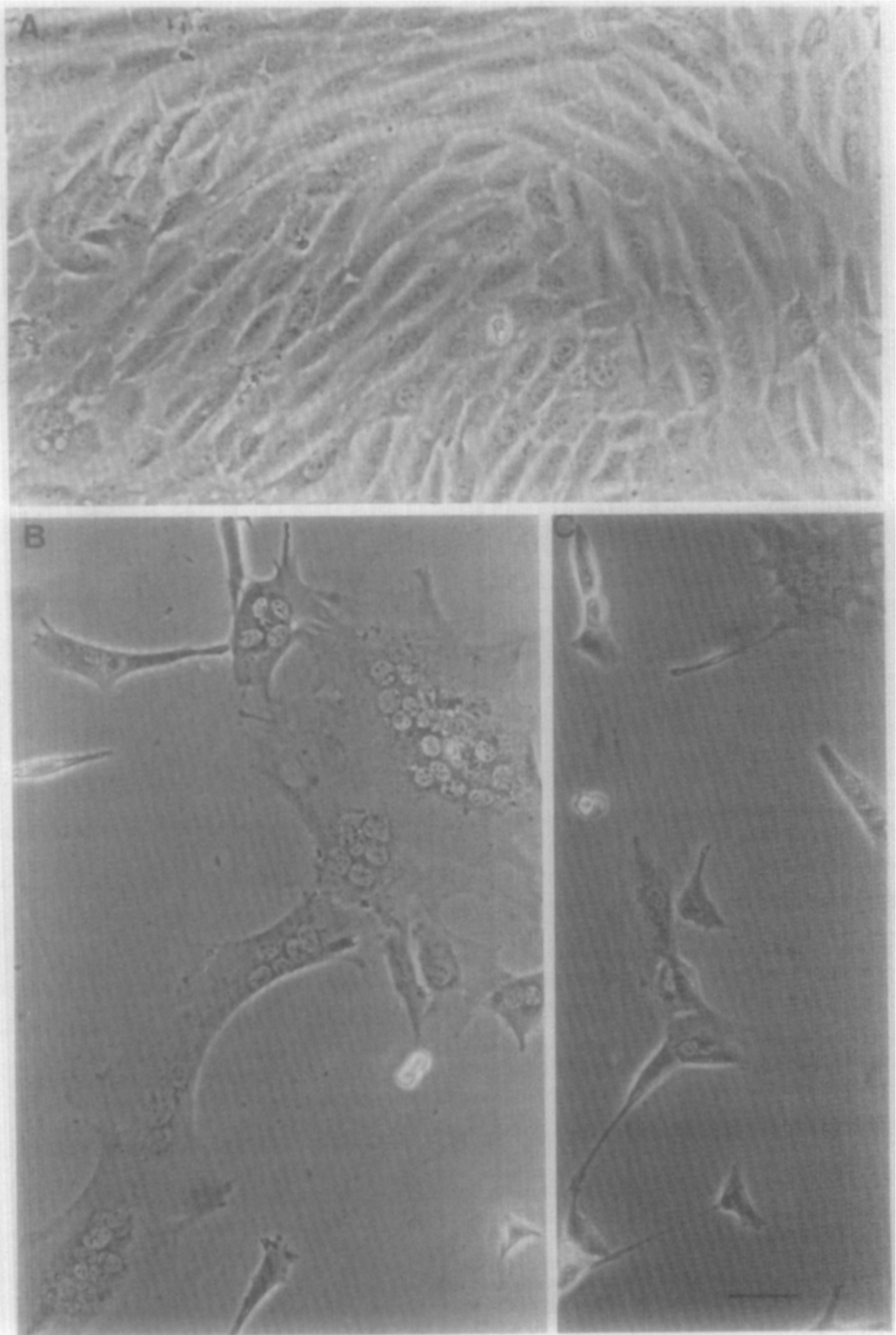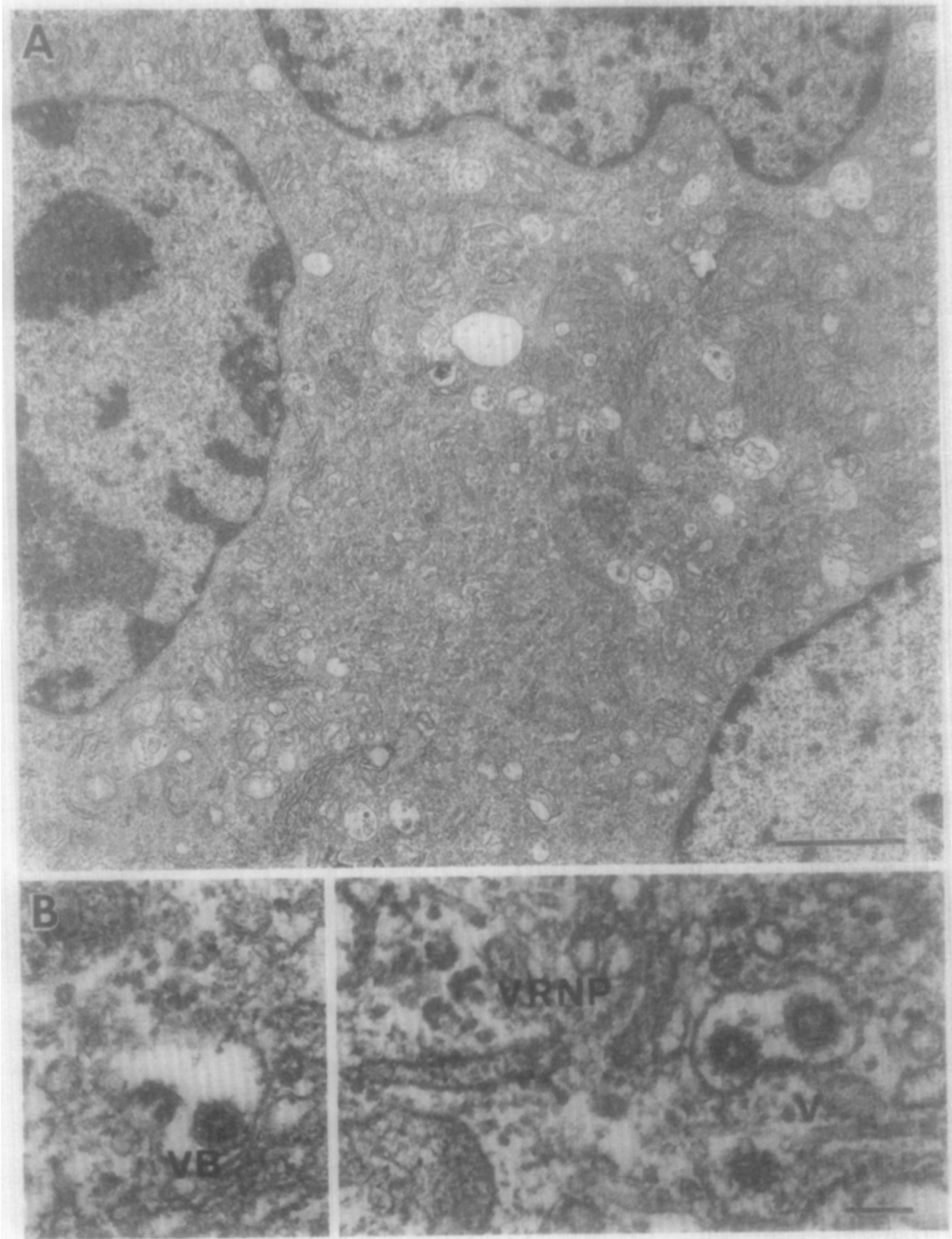
FIG. 5. Transmission electron microscopy of JHMV-infected 17CL-16 cells at 33°. Cells were infected with a m.o.i. of 0.1 and processed for transmission electron microscopy at 8 hpi. (A) demonstrates a typical syncytium. (B) demonstrates viral ribonucleoprotein (VRNP), budding of viral ribonucleoprotein (VB) into a cisterna of the endoplasmic reticulum, and mature virus particles (V) within a cisterna. Scale bar is (A) in 1 μm and in (B) is 100 nm. A59V-infected cells give similar results as do infections at 38.5°.
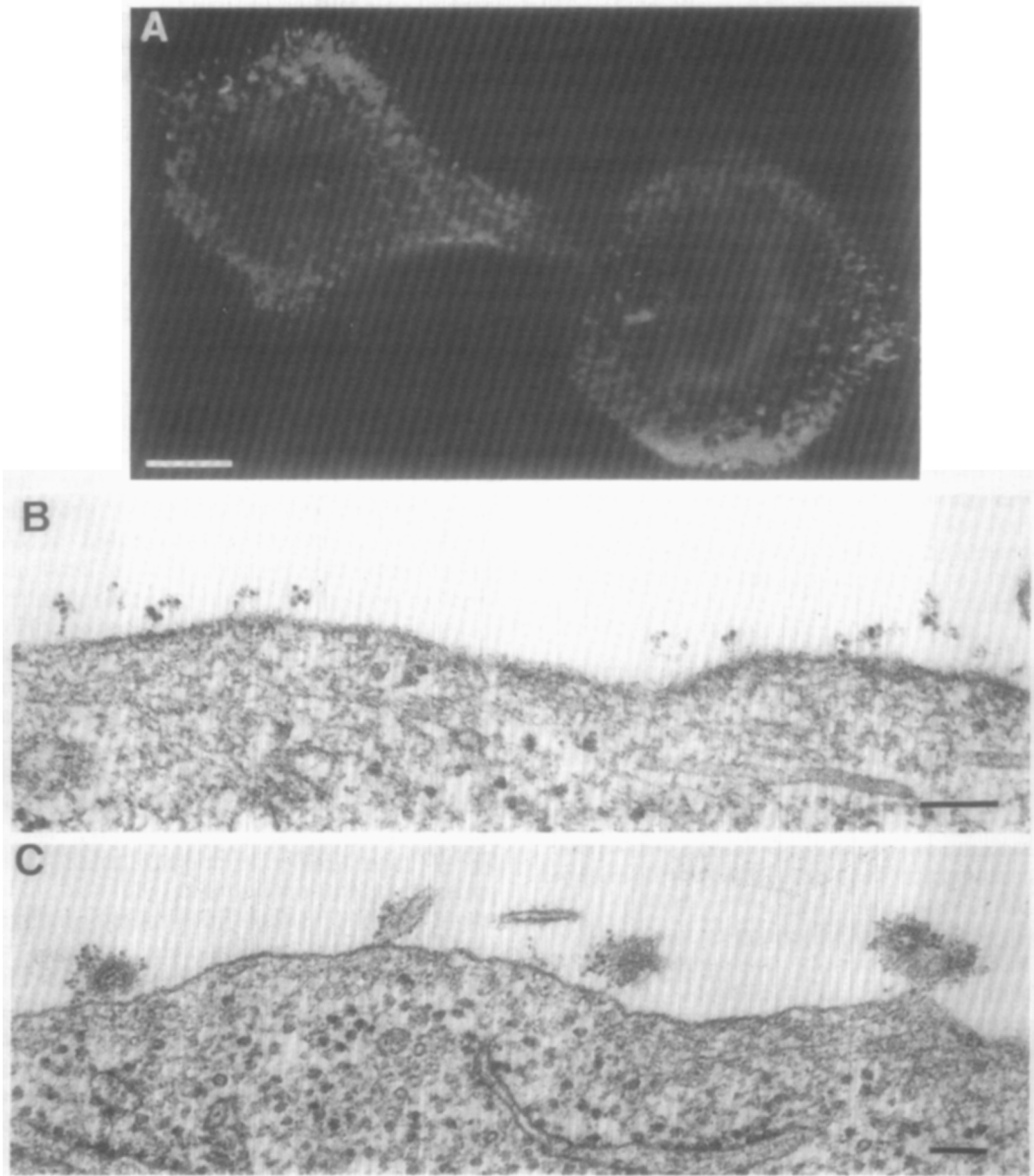
FIG. 6. The presence of JHMV-specific antigen on the surface of living infected 17CL-16 cells. Cells were infected with an m.o.i. of 0.1 and incubated at 38.5° for 4 hr. (A) shows the patchy distribution of the MHMV-specific surface antigen on attached living cells. (B) shows the patchy distribution of the JHMV-specific surface antigen at 3 hpi. Viral ribonucleoprotein has not been identified by transmission electron microscopy anywhere beneath the plasma membrane including the regions containing surface antigen. (C) demonstrates the specificity of the anti-JHMV serum as ferritin-labeled antibody attaches only to the infecting JHMV particles and not to adjacent plasma membrane. Scale bar in (A) is 10 μm and in (B) and (C) is 100 nm. Similar results are obtained using mouse anti-A59V serum and A59V-infected cells. JHMV- and A59V-infected cells give similar results with reciprocal antisera.

FIG. 6. The presence of JHMV-specific antigen on the surface of living infected 17CL-16 cells. Cells were infected with an m.o.i. of 0.1 and incubated at 38.5° for 4 hr. (A) shows the patchy distribution of the MHMV-specific surface antigen on attached living cells. (B) shows the patchy distribution of the JHMV-specific surface antigen at 3 hpi. Viral ribonucleoprotein has not been identified by transmission electron microscopy anywhere beneath the plasma membrane including the regions containing surface antigen. (C) demonstrates the specificity of the anti-JHMV serum as ferritin-labeled antibody attaches only to the infecting JHMV particles and not to adjacent plasma membrane. Scale bar in (A) is 10 μm and in (B) and (C) is 100 nm. Similar results are obtained using mouse anti-A59V serum and A59V-infected cells. JHMV- and A59V-infected cells give similar results with reciprocal antisera.
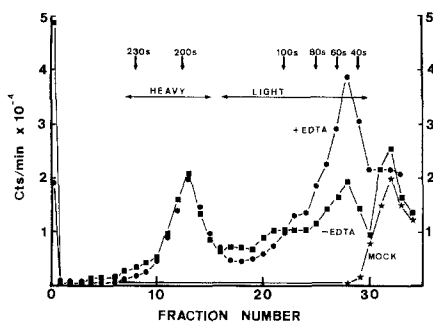
FIG. 7. Analysis of A59V-specific intracellular provirion (nucleocapsid) and messenger ribonucleoprotein (RNP). Cytoplasmic ribonucleoprotein (RNP) synthesized and labeled with [³H]uridine in the presence of 1 μg/ml actinomycin D was extracted with 1% NP40 from mock- and A59V-infected 17CL-16 cells. This extracted RNP was analyzed on a 10–30% equal mass sterile sucrose–RSB gradient. Half of the extracted RNP was treated with 10 mM EDTA (●) before centrifugation (see Materials and Methods for details).

JHMV nucleocapsid has a larger sedimentation value (230 S) than does that of A59V (200 S). This difference has been confirmed in two independent "single-label" experiments using parallel gradients.

Although both viruses synthesis similar amounts of 10–28 S RNA (Fig. 9B), there is considerably less presumptive nucleocapsid RNA made by JHMV. This finding is true throughout the infectious cycle (2–8 hpi at 38.5°) and may be responsible for the reduced yield of infectious JHMV as compared to A59V (10 to 100-fold). Denaturation of the RNA with DMSO had little effect on the RNA profiles (data not shown). Preliminary study of the presumptive nucleocapsid proteins using radioimmune precipitation indicates that at least the major 63,000 (JHMV)- or 60,000 (A59V)-dalton virion protein is present in this EDTA-resistant RNP (see Bond et al., 1979).

DISCUSSION

JHMV is an interesting neurotropic murine coronavirus because it is capable of producing primary demyelination, as well as acute meningoencephalitis, in susceptible weanling mice after intranasal or intra-

cerebral inoculation using low doses of virus. Our approach to understanding the molecular mechanisms underlying the pathogenesis of this JHMV-induced primary demyelination has combined *in vitro* and *in vivo* methods. A detailed molecular description of the replication strategy and virion structure of the murine hepatoencephalitis group of coronaviridae must be achieved before the molecular mechanisms of pathogenesis employed by this group of viruses can be described.

Little is known about the replication strategy of the murine coronaviruses although the structure of the virion is beginning to be explored (Sturman, 1977; Sturman and Holmes, 1977). Our data suggest that the presumptive provirion RNA is a large single-stranded RNA. Preliminary data indicate that at least one tract of polyadenylic acid is present in the virion because two preparations of virion RNA have had over 90% of the deproteinized virion RNA bind to poly(U) Sepharose. Lai and Stohlman (1978) have shown that the virions of A59V and JHMV contain a single-stranded RNA with a molecular weight of 5.4×10^6 daltons. The virion RNAs of MHV-2 (Yogo *et al.*, 1977), JHMV, and A59V (Lai and Stohlman, 1978) contain tracts of polyadenylic acid. The viron RNA of avian infectious bronchitis virus, an avian coronavirus, contains at least one tract of polyadenylic acid and is infectious (Schochetman *et al.*, 1977, Lomniczi, 1977). Furthermore, this avian virion RNA is the largest single-stranded RNA genome yet described in animal virology and is of messenger polarity (Lomniczi and Kennedy, 1977).

Our data indicate that the presumptive mRNA species of both A59V and JHMV are between 10 and 28 S in sedimentation value in sucrose with the dominant species having a value around 18 S. Preliminary analysis of these species with agarose gel electrophoresis suggests that multiple messenger species are present, a finding similar to that with avian infectious bronchitis virus (I. Kennedy, personal communication). If this finding is confirmed the replication strategy of at least the murine and avian
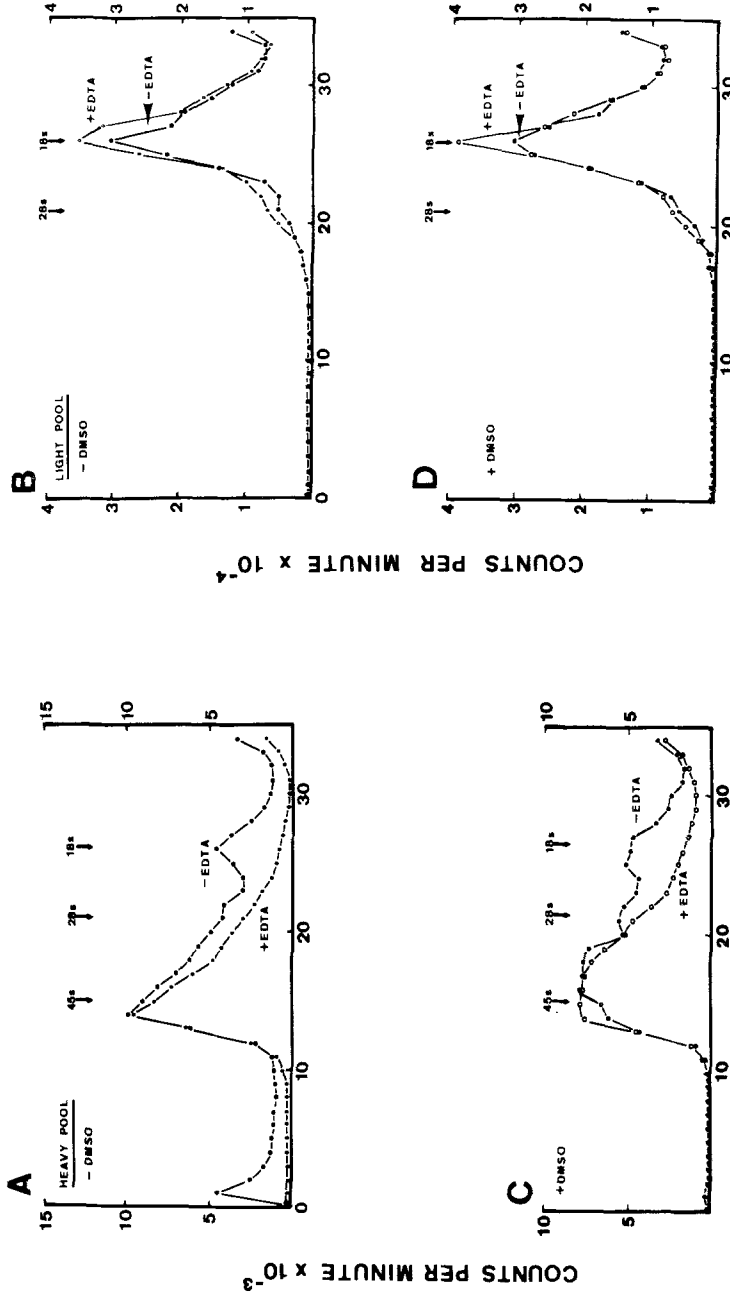
Fig. 8. Analysis of A59V-specific intracellular nucleocapsid and messenger RNA. The "heavy" (A) and "light" (B) pools derived from the gradients shown in Fig. 7 were deproteinized by Proteinase K/cold phenol extraction and analyzed on 10–30% equal mass sucrose–0.1% SDS gradients. Half of each sample of RNA was denatured with DMSO (C and D) before centrifugation (see Materials and Methods for details).
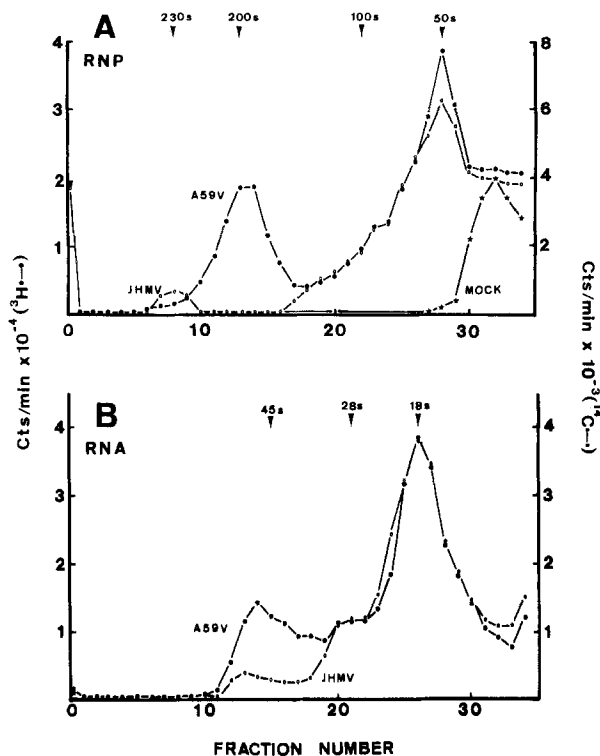
FIG. 9. Analysis of JHMV- and A59V-specific intracellular nucleocapsid and messenger RNP and RNA. Cytoplasmic RNP extracts were prepared and treated with 10 mM EDTA as described in Fig. 7 and under Materials and Methods. A59V- and JHMV-infected cells were labeled with 75 μCi/ml [^{3}H]uridine (●) and 12 μCi/ml [^{14}C]uridine (○), respectively. The RNP extracts were mixed before the addition of EDTA and centrifugation. (A) and (B) demonstrate the RNP and RNA profiles, respectively. Denaturation of the RNA with DMSO had little effect on the RNA profiles (data not shown).

coronaviridae involves a genomic RNA of messenger polarity and a transcriptional mechanism involving probably more than two messengers. This replication strategy would, therefore, be somewhat different from that of the picornaviruses and togaviruses, the other two animal virus groups having a genomic RNA of messenger polarity.

Investigation of the proteins synthesized using purified virus-specific presumptive mRNA species in cell-free translation systems should help to better define the replication strategy of the murine coronaviruses. Comparative biochemistry between the murine and human coronaviruses may be helpful in understanding the molecular mechanisms underlying the pathogenesis of multiple sclerosis (Johnson, 1975; Tanaka et al., 1976) and other demyelinating diseases of the human central nervous system.

REFERENCES

ASH, J. F., and SINGER, S. J. (1976). Concanavalin-A-induced transmembrane linkage of concanavalin A surface receptors to intracellular myosin-containing filaments. *Proc. Nat. Acad. Sci. USA* **73,** 4575–4579.

BAILEY, O. T., PAPPENHEIMER, A. M., CHEEVER, F. S., and DANIELS, J. B. (1949). A murine virus (JHM) causing disseminated encephalomyelitis with extensive destruction of myelin: II, Pathology. *J. Exp. Med.* **90,** 195–221.

BOND, C. W., LEIBOWITZ, J. L., and ROBB, J. A. (1979). Pathogenic murine coronaviruses: II, Characterization of virus-specific proteins of murine coronaviruses JHMV and A59V. *Virology* **94,** 371–384.

CHEEVER, F. S., DANIELS, J. B., PAPPENHEIMER, A. M., and BAILEY, O. T. (1949). A murine virus (JHM) causing disseminated encephalomyelitis with extensive destruction of myelin: I, Isolation and biological properties of the virus *J. Exp. Med.* **90,** 181–194.

EVANS, V. J., EARLE, W. R., WILSON, E. P., WALTZ, H. K., and MACKEY, C. J. (1952). The growth *in vitro* of massive cultures of liver cells. *J. Nat. Cancer Inst.* **12,** 1245–1257.

FENNER, F., and WHITE, D. O. (1976). "Medical Virology." Academic Press, New York.

FREDRICKSON, D. S. (1976). Recombinant DNA research guidelines. *Fed. Regist.* **41,** 27902–27943.

HARLEY, J. W., and ROWE, W. P. (1963). Tissue culture cytopathic and plaque assays for mouse hepatitis viruses. *Proc. Soc. Exp. Biol.* **113,** 403–406.

HUANG, A. S., and BALTIMORE, D. (1970). Defective viral particles and viral disease processes. *Nature (London)* **226,** 325–327.

HERNDON, R. M., PRICE, D. L., and WEINER, L. P. (1977). Regeneration of oligodendroglia during recovery from demyelinating disease. *Science* **195,** 693–694.

HIRANO, N., FUJIWARA, K., HINO, S., and MATUMOTO, M. (1974). Replication and plaque formation of mouse hepatitis virus (MHV-2) in mouse cell line DBT culture. *Arch. Gesamte Virusforsch.* **44,** 298–302.

JOHNSON, R. T. (1975). Virological data supporting the viral hypothesis in multiple sclerosis. *In* "Multiple Sclerosis Research (A. N. Davison and J. H. Humphrey, eds.), pp. 155–183. Elsevier, Amsterdam/New York.

LAI, M. M. C., and STOHLMAN, S. S. (1978). RNA of mouse hepatitis virus. *J. Virol.* **26,** 236–248.

LAMPERT, P. W., JOSEPH, B. S., and OLDSTONE, M. B. A. (1975). Antibody-induced capping of measles virus antigens on plasma membrane studied by electron microscopy. *J. Virol.* **15,** 1248–1255.

LAMPERT, P. W., SIMS, J. K., and KNIAZEFF, A. J. (1973). Mechanism of demyelination in JHM virus encephalomyelitis: Electron microscopic studies. *Acta Neuropathol.* **24,** 76–85.

LOMNICZI, B. (1977). Biological properties of avian coronavirus RNA. *J. Gen. Virol.* **36,** 531–533.

LOMNICZI, B., and KENNEDY, I. (1977). Genome of infectious bronchitis virus. *J. Virol.* **24,** 99–107.

MCINTOSH, K. (1974). Coronaviruses: A comparative review. *Curr. Top. Microbiol. Immunol.* **63,** 86–129.

MONTO, A. S. (1976). Coronaviruses. *In* "Viral Infections of Humans" (Evans, A. S., ed.), pp. 129–130. Plenum, New York.

PENMAN, S., VESCO, C., and PENMAN, M. (1968). Localization and kinetics of nuclear heterodisperse RNA, cytoplasmic heterodisperse RNA and polyribosome-associated messenger RNA in HeLa cells. *J. Mol. Biol.* **34,** 49–69.

PIAZZA, M. (1969). "Experimental Viral Hepatitis." Charles C Thomas, Springfield, Ill.

ROBB, J. A. (1973). Microculture procedures for simian virus 40. *In* "Tissue Culture: Methods and Applications" (P. Kruse and M. K. Patterson, eds.), pp. 517–524. Academic Press, New York.

ROBB, J. A. (1977a). Variation in the appearance of SV40 tumor antigen in transformed cells. *Exp. Cell Res.* **106,** 441–445.

ROBB, J. A. (1977b) Virus-cell interactions: A classification for virus caused human disease. *Progr. Med. Virol.* **23,** 51–61.

ROBB, J. A., and BOND, C. W. (1979). Coronaviridae. *In* "Comprehensive Virology" (H. Fraenkel-Conrat and R. Wagner, eds.), Vol. 14. Plenum, New York, in press.

ROBB, J. A., BOND, C. W., and LEIBOWITZ, J. L. (1979). Pathogenic murine coronavirus: III, Biological and biochemical characterization of temperature-sensitive mutants of JHMV. *Virology* **94,** 385–399.

SCHOCHETMAN, G., STEVENS, R. H., and SIMPSON, R. W. (1977). Presence of infectious polyadenylated RNA in the coronavirus avian bronchitis virus. *Virology* **77,** 772–782.

STURMAN, L. S. (1977). Characterization of a coronavirus: I, Structural proteins: Effects of preparative conditions on the migration of protein in polyacrylamide gels. *Virology* **77,** 637–649.

STURMAN, L. S., and HOLMES, K. V. (1977). Characterization of a coronavirus: II, Glycoprotein of the viral envelope: Tryptic peptide analysis. *Virology* **77,** 650–660.

STURMAN, L. S., and TAKEMOTO, K. K. (1972). Enhanced growth of a murine coronavirus in transformed mouse cells. *Infec. Immun.* **6,** 501–507.

TANAKA, R., IWASAKI, Y., and KOPROWSKI, H. (1976).

Intracisternal virus-like particles in brain of a multiple sclerosis patient. *J. Neurol. Sci.* **28**, 121–126.

TYRRELL, D. A. J., ALMEIDA, J. D., CUNNINGHAM, C. H., DOWDLE, W. R., HOFSTAD, M. S., MCINTOSH, K., TAJIMA, M., ZAKSTELSKAYA, L. YA., EASTERDAY, B. C., KAPIKIAN, A., and BINGHAM, R. W. (1975). Coronaviridae. *Intervirology* **5**, 76–82.

WEINER, L. P. (1973). Pathogenesis of demyelination induced by a mouse hepatitis virus (JHM virus). *Arch. Neurol.* **28**, 298–303.

WIRTH, D. F., KATZ, F., SMALL, B., and LODISH, H. F. (1977). How a single sindbis mRNA directs the synthesis of one soluble protein and two integral membrane glycoproteins. *Cell* **10**, 253–263.

YOGO, Y., HIRANO, N., HINO, S., SHIBUTA, H., and MATUMOTO, M. (1977). Polyadenylate in the virion RNA of mouse hepatitis virus. *J. Biol. Chem.* **82**, 1103–1108.